a = 10.971 (1), b = 11.148 (2), c = 13.943 (1) Å; α = 88.38 (1), β = 78.29 (7), γ = 81.17 (1)°; V = 1650.0 (4) Å^3; cell dimensions determined from 25 reflections with $35 < 2\theta < 45$; Z = 2; D_c = 2.07 Mg m^{-3}; λ = 0.709 30 Å; μ(Mo Kα) = 7.50 mm^{-1}; F(000) = 980 electrons. Crystal dimensions were 0.25 × 0.20 × 0.10 mm.

The intensities of a total of 6112 reflections were measured by the $\theta/2\theta$ method to $2\theta_{max}$ = 47.5°. These were reduced and averaged to yield 5061 unique reflections, of which 2961 were judged observed ($I > 2.0\sigma(I)$). An empirical absorption correction (DIFABS[23]) was applied. Final refinement (by full-matrix methods) used 335 parameters (including an extinction coefficient) and a weighting scheme of the form $w = 1/(\sigma F^2 + 0.001F^2)$. The final R (=$\sum||\Delta F|/\sum|F_o|$) = 0.070, R_w (=$((\sum(w(F_o - F_c)^2)/\sum(wF_o)^2)^{1/2}$) = 0.073, and GoF (=$\sum w(F_o - F_c)^2$/(number of reflections − number of parameters) = 1.474. All non-hydrogen atoms were refined anisotropically; hydrogen atoms were included as fixed contributions (r(C–H) = 0.96 Å, and sp^2 (C_5H_5) or sp^3 ($N(C_2H_5)_3$) geometry), with fixed isotropic thermal parameters equal to that of the C atom to which they were attached. A final difference Fourier had a highest peak of 0.44 e Å^{-3} (located in the Ti_4Se_6 core) and a deepest valley of −0.31 e Å^{-3}. Table II gives the atomic positions for the non-hydrogen atoms; Table I gives important distances and angles. The hydrogen atom positions, the thermal parameters, a comprehensive list of distances and angles, some mean planes, and a list of $|F_o|$ and $|F_c|$ are available in the supplementary material.

X-ray diffraction experiments were made on an Enraf-Nonius CAD4 diffractometer operating under the control of the NRCCAD software.[24] The structure was solved and refined by using the NRCVAX program package.[25] Scattering factors, corrected for anomalous dispersion except in the case of hydrogen, were taken from ref 26.

(23) Walker, N.; Stuart, D. *Acta Crystallogr.* **183**, *A39*, 158.
(24) LePage, Y.; White, P. S.; Gabe, E. J. *Annu. Meet. Am. Cryst. Assoc.*, Hamilton, Ontario, Canada, 1986.
(25) Gabe, E. J.; Lee, F. L.; LePage, Y. In *Crystallographic Computing*; Sheldrick, G. M., Kruger, C., Goddard, R., Eds.; Clarendon Press: Oxford, U.K., 1985; Vol. 3, p 167.
(26) *International Tables for X-ray Crystallography*; Kynoch Press: Birmingham, U.K., 1974; Vol. IV.

Determination of the Structure of $[(\eta\text{-}C_5H_5)_2TiCl]_2(\mu_2\text{-}Se_2)$. Crystal data for $[(\eta\text{-}C_5H_5)_2TiCl]_2(\mu_2\text{-}Se_2)$: M_r = 585.02; orthorhombic, *Pbca*; a = 13.3242 (7), b = 13.9334 (12), c = 22.5441 (18) Å; V = 4185.3 (5) Å^3 (from 24 reflections with $30 < 2\theta < 40°$); Z = 8; D_c = 1.86 Mg m^{-3}; μ(Mo Kα) = 4.46 mm^{-1}; F(000) = 2287.6 electrons. Crystal dimensions were 0.35 × 0.35 × 0.15 mm.

The intensities of a total of 5019 reflections were measured to $2\theta_{max}$ = 50°. These were reduced and averaged to yield 3675 unique reflections, of which only 1734 could be judged as observed by the criteria that $I > 2.0\sigma(I)$. The structure was readily solved in the space group *Pbca* but could not be refined below R = 0.17. A difference Fourier map showed peaks of up to 2.65 e Å^{-3} in the region of the Se and Cl atoms. No better solution was found in the space groups *Pbcm* or *Pbma*. It should be noted that the cell dimensions, space group, and atomic positions found for $[(\eta\text{-}C_5H_5)_2TiCl]_2(\mu_2\text{-}Se_2)$ are very similar to those of the analogous sulfur compound, the structure of which was refined to R = 0.081 with no apparent difficulty.[12] The poor quality of the crystal and the low number of observed reflections (47%) is the probable reason for the inability to refine the structure. It is considered that the diffraction experiments clearly define the major constituent of the crystal as $[(\eta\text{-}C_5H_5)_2TiCl]_2(\mu\text{-}Se_2)$, but further conclusions are not warranted. Accordingly, a list of atomic parameters and other details are given in the supplementary material only.

Acknowledgment. We thank the Natural Sciences and Engineering Research Council of Canada and the donors of the Petroleum Research Fund, administered by the American Chemical Society, for financial support of this work.

Supplementary Material Available: Tables of hydrogen atom positions, thermal parameters for Ti, Se, and C atoms, comprehensive bond distances and angles, and relevant mean planes and atom-numbering diagrams for $[(\eta\text{-}C_5H_5)Ti]_4(\mu_2\text{-}Se)_3(\mu_3\text{-}Se)_3\cdot(C_2H_5)_3N$ and tables of atomic parameters and thermal parameters and an atom-numbering diagram for $[(\eta\text{-}C_5H_5)_2TiCl]_2(\mu\text{-}Se_2)$ (13 pages); tables of $|F_o|$ and $|F_c|$ for both structures (24 pages). Ordering information is given on any current masthead page.

Effect of Molecular Shapes on Crystal Building and Dynamic Behavior in the Solid State: From Crystalline Arenes to Crystalline Metal–Arene Complexes

Dario Braga and Fabrizia Grepioni*

Dipartimento di Chimica "G. Ciamician", University of Bologna, Via F. Selmi 2, 40126 Bologna, Italy

Received November 19, 1990

The molecular organization and dynamic behavior in crystals of C_6H_6 and C_6Me_6 and of the mononuclear complexes $(C_6H_6)_2Cr$, $(C_6H_6)Cr(CO)_3$, $(C_6Me_6)Cr(CO)_3$, and $(1,3,5\text{-}C_6H_3Me_3)Mo(CO)_3$ are investigated by means of packing potential energy calculations and computer graphic analysis, showing that analogies and differences can be rationalized in terms of the shape of the molecules or constituent molecular fragments. Precise relationships are found not only between the crystal packings of these species but also between the shape of the arene fragments and the occurrence of dynamic behavior in the solid state.

Introduction

In spite of the wealth of information contained in the thousands of crystal structures of organometallic compounds characterized up to date, very little is known about the factors that control the organization of organometallic molecules in their crystals and their solid-state properties. While solid-state properties of organic materials have been studied for more than 30 years[1,2] (and are a matter of continuing investigation), no systematic study of organometallic crystal structures has, until now, appeared in the scientific literature.

(1) *Organic Solid State Chemistry*; Desiraju, G. R., Ed.; Elsevier: New York, 1987.
(2) Kitaigorodsky, A. I. *Molecular Crystal and Molecules*; Academic Press: New York, 1973.

0276-7333/91/2310-2563$02.50/0

It is important to appreciate that a detailed knowledge of the molecular environment in the crystal and of the forces at work among the molecules is the ground on which the understanding of phenomena such as phase transitions, small and large amplitude motions, and reorientations (in general dynamic behavior), let alone the crystallization process itself and the reactivity in the solid state, must be founded.[3]

In previous papers[4] we have investigated the crystal packing of neutral metal binary carbonyls and the molecular self-recognition process on which the crystal building of low nuclearity carbonyl clusters is based. The atom–atom pairwise potential energy method,[5] developed and still widely used in the organic solid-state chemistry field, has been successfully applied.

In this paper, we focus our attention on the *changes* in packing motives and molecular organization which occur when a given organic fragment, present as an individual molecule in its crystal, is coordinated to a metal center. To this purpose, we have chosen to study the relationship between crystals of benzene and hexamethylbenzene and those of the corresponding mononuclear Cr complexes $(C_6H_6)_2Cr$, $(C_6H_6)Cr(CO)_3$, and $(C_6Me_6)Cr(CO)_3$. These complexes represent appropriate "test-cases" since their solid-state structures and dynamic behaviors have been the subject of considerable spectroscopic and crystallographic work. For example, the reorientational motion of the metal-bound arene fragments in the solid state has been extensively studied by NMR techniques (see below). The unusual case of $(C_6H_3Me_3)Mo(CO)_3$ will also be examined.

The aims of the paper can be summarized as follows: (i) to investigate the relationship between the *shape* of small organic molecules, such as C_6H_6 and C_6Me_6, and that of the corresponding metal complexes mentioned above, and the role of molecular shape in determining the molecular organization in the crystal lattices; (ii) to verify whether the shapes of simple molecular fragments [such as C_6H_6, C_6Me_6, and $(CO)_3$] can be treated as *transferable properties* ("shape elements") on going from one crystalline organometallic species to another; (iii) to correlate the dynamic behavior shown by the aforementioned metal complexes in the solid state to the shape of the constituent fragments. The possibility of "predicting" the occurrence of reorientational motions simply from the knowledge of the geometry of the molecular fragments will also be discussed.

Methodology

The packing potential energy (ppe) of organometallic crystals composed of neutral species can be evaluated within the atom–atom pairwise potential energy method[5] by means of the expression

$$\text{ppe} = \sum_i \sum_j [A \exp(-Br_{ij}) - Cr_{ij}^{-6}]$$

where r_{ij} represents the nonbonded atom–atom intermolecular distance. Index i in the summation runs over all atoms of one molecule (chosen as reference molecule, RM) and index j over the atoms of the surrounding molecules distributed according to crystal symmetry. A cutoff of 10 Å has been adopted in our calculations. The values of the coefficients A, B, and C used in this work are listed in Table I.[6] The Cr and Mo atoms, for which

Table I. Parameters for the Atom–Atom Potential Energy Calculations[a]

	A, kcal mol^{-1}	B, Å^{-1}	C, kcal mol^{-1} Å^6
H···H	4900	4.29	29.0
C···C	71600	3.68	421.0
O···O	77700	4.18	259.4
Cr···Cr[b]	270600	3.28	3628.0
Mo···Mo[b]	372900	3.03	8373.0

[a] For crossed interactions: $A = (A_xA_y)^{1/2}$, $B = (B_x + B_y)/2$, $C = (C_xC_y)^{1/2}$. [b] Cr···Cr and Mo···Mo interactions were treated as Kr···Kr and Xe···Xe interactions, respectively (see text).

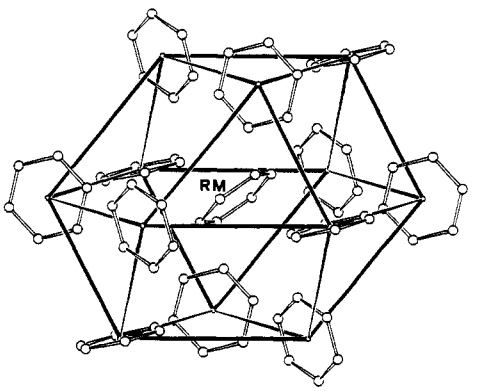

Figure 1. The cubooctahedral ES of benzene showing the distribution of the 12 first neighboring molecules around RM (H atoms are omitte for clarity).

such coefficients are not available, are treated as the corresponding noble gases (Kr and Xe). Ionic contribution are not considered. We have found that this choice of potential coefficients performs well when dealing with mononuclear or polynuclear organometallic complexes containing only O, C, and H atoms beside the metal ones.[7]

The results of ppe calculations are used to investigate the molecular packing arrangement around the reference molecule (RM).[4] First, the separate contributions to ppe of all the molecules (usually in number from 50 to 80) having at least one atom falling within the cutoff distance of 10 Å, generated around RM by space group symmetry, are calculated. Then the first neighboring molecules (those constituting the enclosure shell, ES hereafter) are selected on the basis of the highest number of intermolecular contacts with RM. This procedure ensures that all relevant contributions to ppe are taken into account.

It should be stressed, however, that the pairwise potential energy method is used herein *only* as a means (more efficient than others, though) to investigate the spatial distribution of the molecules around the one chosen as reference, with no pretentions of obtaining "true" crystal potential energy values. Details of the application of the method to organometallic crystals are given in refs 4 and 7.

Packing coefficients (pc) are calculated from the ratio $(V_{mol}Z)/V_{cell}$, where V_{mol} is the van der Waals volume of the molecule calculated by the method of the "intersecting caps" of Kitaigorodsky.[2b] The following values were used for the van der Waals radii: H, 1.17; C, 1.75; O, 1.52; Cr, 2.15; Mo, 2.35 Å.[8] In view of the uncertainty on the metal atom van der Waals radii, the discussion of the pc values is useful only on a *relative basis*, i.e. for comparison between closely related systems. All calcu-

(3) Gavezzotti, A.; Simonetta, M. *Chem. Rev.* **1982**, *82*, 1 and references therein.
(4) Braga, D.; Grepioni, F.; Sabatino, P. *J. Chem. Soc., Dalton Trans.* **1990**, 3137. Braga, D.; Grepioni, F. *Organometallics* **1991**, *10*, 1254.
(5) Pertsin, A. J.; Kitaigorodsky, A. I. *The atom-atom potential method*; Springer-Verlag: Berlin, 1987.
(6) (a) Gavezzotti, A.; *Nouv. J. Chim.* **1982**, *6*, 443. (b) Mirsky, K. Computing in Crystallography. *Proceedings of the International Summer School on Crystallographic Computing*; Delf University Press: Twente, 1978; p 169.
(7) (a) Braga, D.; Gradella, C.; Grepioni, F. *J. Chem. Soc., Dalton Trans.* **1989**, 1721. (b) Braga, D.; Grepioni, F. *Polyhedron* **1990**, *1*, 53. (c) Braga, D.; Grepioni, F.; Johnson, B. F. G.; Lewis, J.; Martinelli, M. *J. Chem. Soc., Dalton Trans.* **1990**, 1847. (d) Braga, D.; Grepioni, F. *J. Chem. Soc., Dalton Trans.* **1990**, 3143.
(8) Bondi, A. *J. Phys. Chem.* **1964**, *68*, 441. See also: Braga, D.; Grepioni, F. *Acta Crystallogr., Sect. B* **1989**, *45*, 378.

Table II. Summary of Crystal and Molecular Qualifiers[a]

species	space group	ppe	pc	$E_{arene-arene}$	$E_{arene-CO}$	E_{CO-CO}	contr[b]
$(C_6H_6)_2Cr$	$Pa\bar{3}$	-43.5	0.54	-17.3			63%
$(C_6H_6)Cr(CO)_3$	$P2_1/m$	-35.5	0.57	-7.0	-8.0	-4.0	47%
$(1,3,5\text{-}C_6H_3Me_3)Mo(CO)_3$	$P2_1/c$	-45.1	0.60	-15.0	-7.7	-3.5	42%
$(C_6Me_6)Cr(CO)_3$	$Pbca$	-46.7	0.64	-19.1	-10.0	-1.3	36%

[a] Ppe, $E_{arene-arene}$, $E_{arene-CO}$, E_{CO-CO} are expressed in kcal mol^{-1}. [b] Metal contribution = (E_{metal}/ppe) × 100.

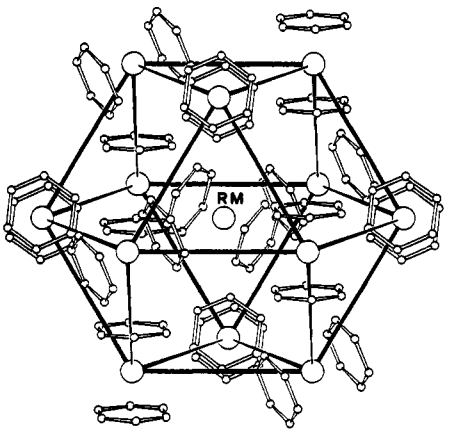

Figure 2. The cubooctahedral ES of $(C_6H_6)_2Cr$ showing the distribution of the 12 first neighboring molecules around RM (H atoms are omitted for clarity).

lations were carried out with the aid of the computer program OPEC;[9] SCHAKAL88[10] was used for the graphical representation of the results.

The basic information on the crystal and molecular qualifiers relevant for the following discussion are collected in Table II.

Results and Discussion

From Benzene to Bis(benzene)chromium. As clearly described by Cox and Cruickshank in 1958,[11a] the benzene molecules fit in its crystal lattice with almost perpendicular ring planes (90.3°). According to the more recent classification put forward by Gavezzotti and Desiraju,[12] the molecular packing of benzene is of the "herringbone" type, a feature shared with many fused aromatic hydrocarbons such as naphthalene, anthracene, phenanthrene, etc.

Cox and Cruickshank described the molecular environment around a benzene molecule as constituted of 12 near neighbors. As shown in Figure 1, the centers of these 12 molecules define a slightly distorted cubooctahedral ES around the central benzene molecule (the reference molecule, RM).

The ES approach allows one to see that there is a strict relationship between the molecular arrangements in crystalline benzene and $(C_6H_6)_2Cr$ [note that benzene crystallizes in the space group *Pbca* with a = 7.39, b = 9.42, c = 6.81 Å (at -135 °C), while $(C_6H_6)_2Cr$ crystallizes in the space group $Pa\bar{3}$ with $a = b = c$ = 9.67 Å].[13] As a matter of fact the first neighboring molecules around the reference $(C_6H_6)_2Cr$ molecule generate a cubooctahedral ES (see Figure 2) which closely resembles that of benzene.

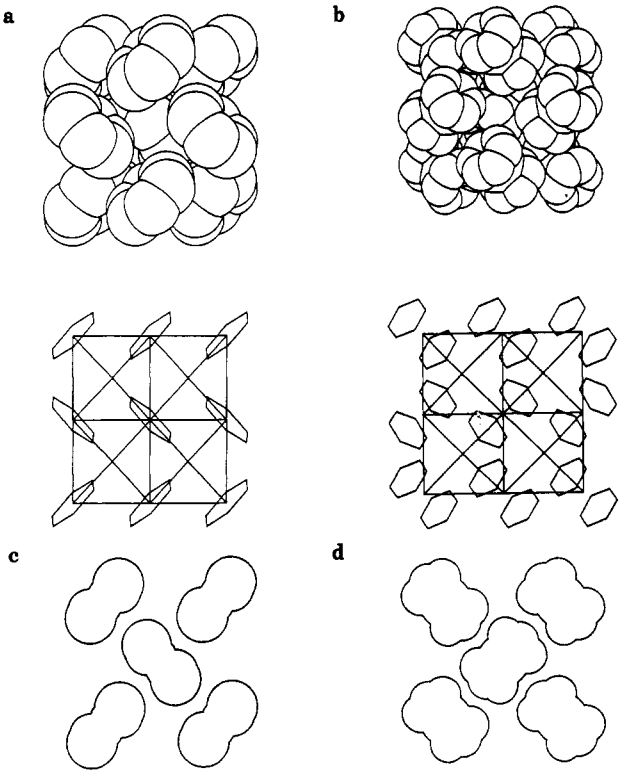

Figure 3. Parts a and b show space-filling (top) and stick (bottom) projections of the ESs of C_6H_6 and $(C_6H_6)_2Cr$ perpendicular to the unit cell b axes; parts c and d show grid cutting through the central layers of a (top) and b (top).

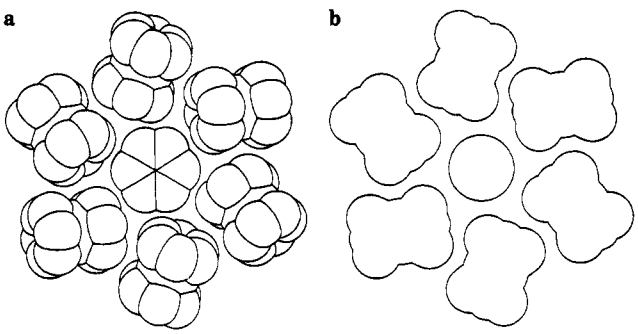

Figure 4. Space-filling (a) and grid-cutting (b) of the equatorial plane perpendicular to the molecular axis of $(C_6H_6)_2Cr$ showing the arrangement of the six first neighboring molecules (H atoms are omitted for clarity).

Therefore, *both* benzene *and* $(C_6H_6)_2Cr$ adopt a pseudocubic closest-packed arrangement in their crystals (ABC sequence of layers).

The similarity between the crystals of benzene and $(C_6H_6)_2Cr$ is not confined to the ESs. Figure 3, parts a and b show a projection perpendicular to the unit cell b axis of the benzene and $(C_6H_6)_2Cr$ ESs [note, incidentally, that the length of the unit cell b axis of benzene is very similar to the unit cell axes of $(C_6H_6)_2Cr$]. It can be easily appreciated that the C_6H_6 planes in the two projections have similar relative orientations. This analogy is better evi-

(9) Gavezzotti, A. *OPEC, Organic Packing Potential Energy Calculations*; University of Milano, Italy. See also: Gavezzotti, A. *J. Am. Chem. Soc.* **1983**, *195*, 5220.

(10) Keller, E. *SCHAKAL88, Graphical Representation of Molecular Models*; University of Freiburg: FRG, 1988.

(11) (a) Cox, E. G.; Cruickshank, D. W. J.; Smith, J. A. S. *Proc. R. Soc. London, Ser. A* **1958**, *247*, 1. (b) Bacon, G. E.; Curry, N. A.; Wilson, S. A. *Proc. R. Soc. London, Ser. A* **1964**, *279*, 98.

(12) Gavezzotti, A.; Desiraju, G. R. *Acta Crystallogr., Sect. B* **1988**, *B44*, 427.

(13) Keulen, E.; Jellinek, F. *J. Organomet. Chem.* **1966**, *5*, 490.

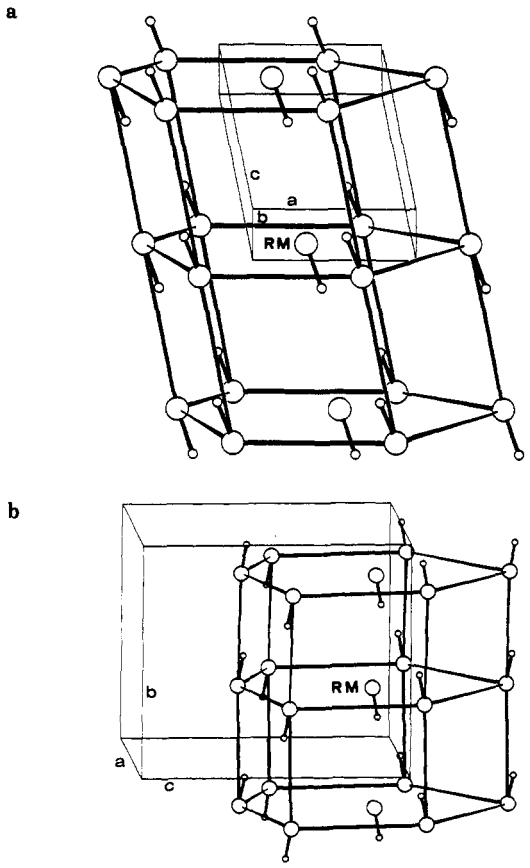

Figure 5. The ESs of $(C_6H_6)Cr(CO)_3$ (a) and $(C_6Me_6)Cr(CO)_3$ (b) showing the stacking sequence of approximately hexagonal layers and the orientation of the unit cells. The $(CO)_3$ and arene groups are omitted for clarify; the small circles represent the midpoints of the C_6 rings.

denced in Figure 3, parts c and d, which show the result of cutting a grid of the central layers perpendicular to the *b* axes: in both cases the central molecule is surrounded by four first neighbors at ca. 90° angles. These views provide strong evidence for the claim that the packing in $(C_6H_6)_2Cr$ is essentially dictated by the disk-like shape of the arene fragment and by its spatial requirements.

Because of the presence of the Cr atom sandwiched between the two benzene ligands, the overall shape of a $(C_6H_6)_2Cr$ molecule is that of a cylinder only in first approximation. The molecule presents a hollow region around the metal atom sandwiched between the two benzene ligands which is used for molecular self-assembling in the crystal lattice. Figure 4a shows a space-filling projection of the ES equatorial plane perpendicular to the axis passing through the Cr atom and the centers of the two benzene rings. It can be seen that each surrounding molecule "pushes in" one of its C–H groups to fill up the recess around the Cr atom. The hexagonal symmetry of the molecule is responsible for the peculiar propeller-like distribution of the surrounding molecules (Figure 4b).

From $(C_6H_6)_2Cr$ to $(C_6H_6)Cr(CO)_3$ and $(C_6Me_6)Cr(CO)_3$. The effect of the presence of a $(CO)_3$ group on the molecular organization in the lattice can now be examined by considering the crystal packing of $(C_6H_6)Cr(CO)_3$[14] and $(C_6Me_6)Cr(CO)_3$.[15] With respect to $(C_6H_6)_2Cr$, the substitution of one tricarbonyl group for a benzene fragment results in the simultaneous presence of a flat fragment with 6-fold symmetry and of a conical fragment with 3-fold

(14) Bailey, M. F.; Dahl, L. F. *Inorg. Chem.* **1965**, *4*, 1314.
(15) Bailey, M. F.; Dahl, L. F. *Inorg. Chem.* **1965**, *4*, 1298.

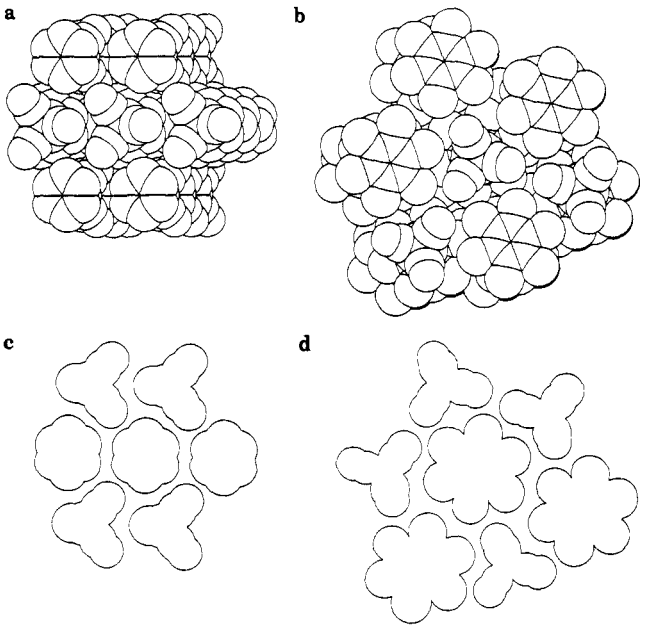

Figure 6. Parts a and b show space-filling views of the molecular "piles" in $(C_6H_6)Cr(CO)_3$ and $(C_6Me_6)Cr(CO)_3$, respectively; parts c and d show grid cutting through the central arene plane showing the first neighboring molecules around the arene fragments in $(C_6H_6)Cr(CO)_3$ and $(C_6Me_6)Cr(CO)_3$.

symmetry. Figure 5, parts a and b show the ESs of $(C_6H_6)Cr(CO)_3$ and $(C_6Me_6)Cr(CO)_3$, respectively. They are closely related and can be discussed together. Both ESs can be seen as constituted of stacking sequences of approximately hexagonal layers, with RMs surrounded by a total of 20 molecules. This molecular distribution differs very much not only from that of $(C_6H_6)_2Cr$ discussed above, but also from that of $Cr(CO)_6$, whose ES was found to contain 12 molecules and could be described as a piece of hcp.[4a]

Differences between $(C_6H_6)Cr(CO)_3$ and $(C_6Me_6)Cr(CO)_3$ arise when the relative orientations of the molecules with respect to the RMs are examined. Figures 6, parts a and b show a view of the molecular piles perpendicular to the layers. It can be seen that: (i) in both crystals the arene groups intermix with the $(CO)_3$ groups belonging to molecules in inverted orientation; (ii) while in $(C_6H_6)Cr(CO)_3$ the arene and $(CO)_3$ groups form parallel rows, in $(C_6Me_6)Cr(CO)_3$ the two fragments form a chevron-like pattern; (iii) in both cases, however, each arene group is surrounded by two other arene units and by four $(CO)_3$ ones (therefore each $(CO)_3$ group is surrounded by four arene groups and by two $(CO)_3$ ones). This can be better appreciated from Figures 6, parts c and d, which show the result of cutting a grid through the arene layers.

It appears that the best way to pack together disk-like fragments with 6-fold symmetry and cone-like fragments with 3-fold symmetry is to have the molecules piled in rods. The way in which such rods intermix depends on the diameter of the disks. In $(C_6Me_6)Cr(CO)_3$, where the C_6Me_6 fragment is (in projection) much larger than the $(CO)_3$ one, optimization of the interlocking between the two fragments is achieved by placing the $(CO)_3$ group in the small cavity left among four (C_6Me_6) groups.

A comparison of the packing coefficients of $(C_6H_6)Cr(CO)_3$ and $(C_6Me_6)Cr(CO)_3$ (see also next section and Table II) indicates that a better space-filling is achieved in crystals of the latter than of the former species (pcs are 0.64 and 0.57, respectively).

Finally, it is enlightening to compare the molecular assemblage in crystalline $(C_6Me_6)Cr(CO)_3$ with that of C_6Me_6

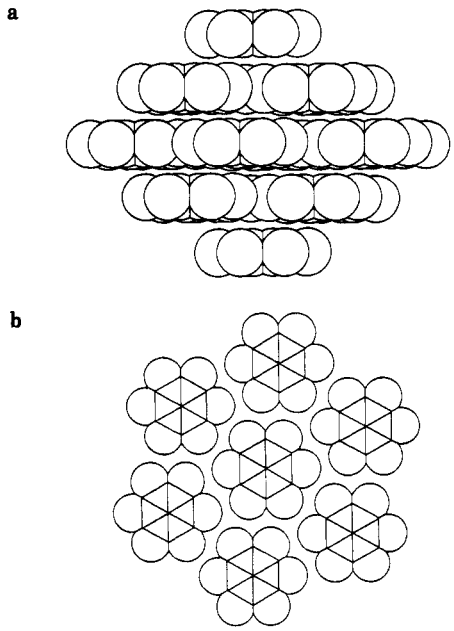

Figure 7. C_6Me_6: (a) projection parallel to the layers and (b) space-filling projection of a layer of molecules.

as a free molecule.[16] A projection perpendicular to the cell *c* axis of this latter crystal is shown in Figure 7a, while a space-filling projection of a layer of molecules is shown in Figure 7b. Beside the interesting graphite-like molecular arrangement (which, obviously, can not be maintained in the Cr complex) it is noticeable that the arene groups in both crystalline C_6Me_6 and $(C_6Me_6)Cr(CO)_3$ adopt a similar, coplanar distribution.

The Case of $(1,3,5\text{-}C_6H_3Me_3)Mo(CO)_3$. $(1,3,5\text{-}C_6H_3Me_3)Mo(CO)_3$[17] is one of a very few examples of eclipsed (arene)$M(CO)_3$ complexes (M = Cr, Mo) (the vast majority shows a staggered conformation,[18] notable exceptions being also $(C_6H_5Me)Cr(CO)_3$[19] and $(C_6Et_6)Cr/Mo(CO)_3$[20]). Our interest arises from the observation that $(1,3,5\text{-}C_6H_3Me_3)Mo(CO)_3$ is made up of two fragments with 3-fold symmetry bound to the metal center. Due to the eclipsed conformation, the overall molecular shape can be seen as a sort of trigonal prism or truncated trigonal pyramid. Such a shape can be expected to have rather different spatial requirements with respect to those discussed so far. This is indeed so. The ES of $(1,3,5\text{-}C_6H_3Me_3)Mo(CO)_3$ is shown in Figure 8a, together with the unit cell, and can be described as a stacking sequence of ABCD(A) layers. The spacing between layers A and B, and C and D, is very small (3.14 Å) and almost half of the spacing between layers B and C (5.40 Å). It can be noticed that: (i) the $(CO)_3$ groups efficiently interlock along their 3-fold axes (see Figure 8b), generating a sort of "dimeric" $[(C_6H_3Me_3)Mo(CO)_3]_2$ unit; (ii) the $(CO)_3\cdots(CO)_3$ interlocking brings the Mo atoms in close proximity (Mo···Mo 5.66 Å) and is responsible for the closeness of the AB and CD layer pairs; (iii) the arene fragments, due to their triangulated shape, interact by lying their edges almost perpendicular to the flat surface of neighboring arenes.

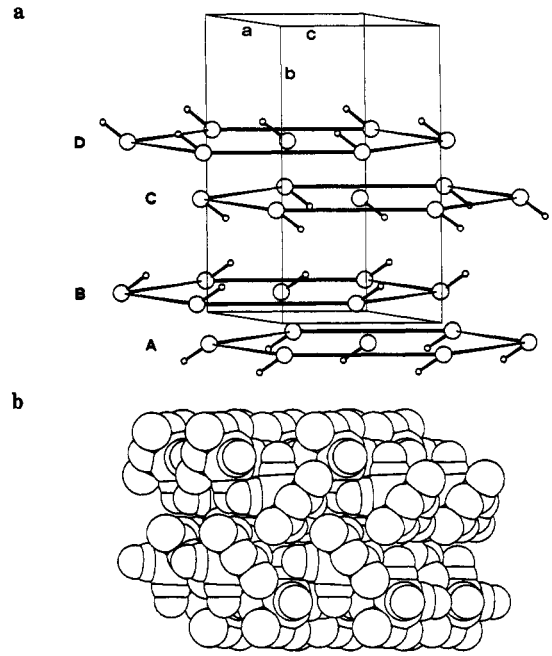

Figure 8. (a) The ES of $(1,3,5\text{-}C_6H_3Me_3)Mo(CO)_3$ showing the ABCD stacking sequence of layers (the small circles represent the midpoint of the C_6-rings). (b) A side view showing the $(CO)_3\cdots(CO)_3$ interlocking and the "herringbone" distribution of the arene fragments.

The arene distribution recalls the "herringbone" pattern discussed above.

Thus, the molecular interlocking in crystalline $(1,3,5\text{-}C_6H_6Me_3)Mo(CO)_3$ is totally different from that of $(C_6H_4)Cr(CO)_3$ and $(C_6Me_6)Cr(CO)_3$. It may well be that the eclipsed conformation is preferred to the staggered one because the former leads to a more efficient assemblage of these two fragments in the solid state. On the other hand, it is well known that the energy differences between the two conformations is very small as documented by both experimental and theoretical studies on $(C_6H_6)Cr(CO)_3$ and a number of related species,[21] so that the self-assembling requirements of the conical $(CO)_3$ and triangular $(C_6H_3Me_3)$ fragments might control the conformational choice in the solid state. A definite answer to this question, however, will probably come only when (and if) it will be possible to *calculate* the most stable crystal packing for an organometallic molecule.

Comments on the Molecular Qualifiers. The data collected in Table II lead to the following observations:

(i) The packing coefficient (pc) of $(C_6H_6)_2Cr$ is much smaller than that of the (arene)$M(CO)_3$ species. For these latter species, pc values increase on increasing the number of methyl groups on the arenes, i.e. the tightest packing, in terms of volume occupation efficiency, is achieved by $(C_6Me_6)Cr(CO)_3$ (pc 0.64).

(ii) Ppe follows a similar trend, showing an increase in cohesion (i.e. "more negative" values) on increasing the arene size. Note that the ppe value of $(C_6H_6)_2Cr$ is much larger (in absolute value) than that of $(C_6H_6)Cr(CO)_3$ (−43.5 and −35.5 kcal mol^{-1}, respectively). In the present case this is due not only to the larger number of atoms (25 versus 19) but also to the fact that, with respect to $(C_6H_6)_2Cr$, the C(CO) atoms in the carbonyl species are closer to the metal atom and further away from the surrounding molecules. This can be substantiated by partitioning the ppe into the separate arene–arene and $(CO)_3$–$(CO)_3$ contributions:

(16) Brockway, L. O.; Robertson, J. M. *J. Chem. Soc.* **1939**, 1324.
(17) Koshland, D. E.; Myers, S. E.; Chesick, J. P. *Acta Crystallogr., Sect. B* **1977**, *B33*, 2013.
(18) Muetterties, E. L.; Bleeke, J. R.; Wucherer, E. J.; Albright, T. A. *Chem. Rev.* **1982**, *82*, 499.
(19) Van Meurs, F.; Van Konigsveld, H. J. *J. Organomet. Chem.* **1977**, *131*, 423.
(20) Iverson, D. J.; Hunter, G.; Blount, J. F.; Damewood, J. R. Jr.; Mislow, K. *J. Am. Chem. Soc.* **1981**, *103*, 6073.
(21) Albright, T. A.; Hofmann, P.; Hoffmann, R. *J. Am. Chem. Soc.* **1977**, *99*, 7546. Albright, T. A. *Acc. Chem. Res.* **1982**, *15*, 149.

Table III. Comparison of E_a and ΔE Values[26] (kcal mol^{-1}) for Arene Reorientation in the Solid State

	^{1}H NMR T_1 measurement: E_a	ref	ΔE	ref
C_6H_6	3.7–4.2	27	3.6 (218 K), 5.4 (138 K)	28
$(C_6H_6)_2Cr$	"free rotation"	29	2.0 (room temp), 3.9 (100 K)	8b
$(C_6H_6)Cr(CO)_3$[a]	4.2 (77–300 K)	30	4.6 (room temp), 7.5 (78 K)	8b
C_6Me_6	6.7 (>150 K)	31	3.0 (room temp)	28
$(C_6Me_6)Cr(CO)_3$	6.2 (183–396 K)	32	3.4 (room temp)	32

[a] To be compared also with data from Raman (4.7 at 300 K, 6.2 at 120 K)[25a] and IQENS (3.7 at 300 K).[25b]

while the former increase on going from $(C_6H_6)Cr(CO)_3$ to $(1,3,5\text{-}C_6H_3Me_3)Mo(CO)_3$ and to $(C_6Me_6)Cr(CO)_3$ (−7.0, −15.0, and −19.1 kcal mol^{-1}), the latter decrease (−4.0, −3.5, and −1.3 kcal mol^{-1});

(iii) However, the *average* contribution to ppe of the CO groups falls in the narrow range −3.9/−4.5 kcal mol^{-1} in agreement with the homomeric principle,[22] which states that a given group of atoms tends to give a constant contribution to ppe irrespective of the molecular and crystal structure.

(iv) The metal atom contribution also decreases, passing from 63% of the total ppe in $(C_6H_6)_2Cr$ to 36% in $(C_6Me_6)Cr(CO)_3$ in agreement with the fact that the metal atoms are progressively further apart with increasing overall molecular size (the homomeric principle applies only to atoms on the periphery of the molecular frame).

Dynamic Behavior in the Solid State and Conclusions. The occurrence of reorientational motions of organic and organometallic molecules in the solid state is well established.[23] Such dynamic phenomena are usually studied by ^{1}H wide-line NMR or ^{13}C CP/MAS NMR spectroscopy and by potential energy barrier calculations based on the same Buckingham potential function used to compute packing potential energies.[7,24] Raman spectroscopy and quasiinelastic neutron scattering (IQENS) have also been used in a variety of cases.[25] The results of these different approaches are often in very good agreement.

The literature values of the activation energies (E_a) and of the potential energy barriers (ΔE) to arene reorientation in solid C_6H_6, $(C_6H_6)_2Cr$, $(C_6H_6)Cr(CO)_3$, C_6Me_6, and $(C_6Me_6)Mo(CO)_3$ are collected in Table III.

Both sources of dynamic information indicate that arene reorientation encounters low potential energy barriers for all species listed in the table.[26] Furthermore, there is no appreciable difference between the dynamic behavior of benzene and hexamethylbenzene, or between $(C_6H_6)Cr(CO)_3$ and $(C_6Me_6)Cr(CO)_3$. On the other hand, reorientation of the arene ligand in solid $(C_6H_3Me_3)Mo(CO)_3$ can not take place at room temperature ($\Delta E > 50$ kcal mol^{-1}).[33] This is not surprising: a rotational motion of the arene around its coordination axis would lead the methyl groups to clash against the flat surface of a neighboring fragment. It is worth noting here also that a large barrier to molecular reorientation (87.75 kcal mol^{-1}) has also been reported in crystalline $(1,3,5\text{-}C_6H_3Cl_3)$.[28]

The observation that the activation energies/potential barriers for the reorientational processes in solid benzene and hexamethylbenzene are strictly comparable to the values obtained for the corresponding metal tricarbonyl complexes indicates that the intermolecular interactions due to crystal packing exert a similar control on the dynamic behaviors of these fragments *whether as free molecules or coordinated to metal centers*. This is an important indication that, in crystalline organometallic species, the extent of reorientation is a *transferable property* which depends primarily on the *shape* of the fragment (given that the bonding interactions are substantially delocalized *and* that the intramolecular nonbonding ones do not "lock in" the fragment).

In other words, it appears that the occurrence of a dynamic behavior depends strictly on the spatial requirements of the particular fragment under examination ("shape factor") and not on other crystalline properties. Thus a disk-like fragment with a regular border shape (like benzene and hexamethylbenzene and also cyclopentadienyl, hexahalogenated benzenes, etc.) is expected to be able to rotate easily in any crystal structure (given the bonding conditions stated above) while a "shape element" presenting cavities and bumps, or protruding groups (as in mesitylene or toluene), will more readily interlock with neighboring molecules. Support for this way of thinking comes from our earlier observation that in crystalline $(C_6H_5Me)M(CO)_3$ [M = Cr, Mo] the toluene fragment is unable to rotate freely at room temperature, being able to undergo only large amplitude oscillatory motion around the molecular coordination axis.[7b,d] Similarly, the arene fragments in $(1,2,4,5\text{-}C_6H_2Me_4)Cr(CO)_3$ and $(1,2,3\text{-}C_6H_3Me_3)Cr(CO)_3$ have been shown to reach a true reorientational state only above ca. 330 K, where a phase transition occurs.[32] On the other hand, rotational freedom at room temperature has been observed for the (C_5H_5) ligand in both cis and trans isomers of $(C_5H_5)_2Fe(CO)_4$ in agreement with the results of ^{13}C MAS NMR experiments. Obviously there is no precise borderline between reorientational and large amplitude oscillatory motions, and a continuum of dynamic behavior from small-amplitude libration to rotational freedom, via intermediate large-amplitude motion, can be expected to be seen on varying the fragment shape.

In conclusion, the observation that chemically different molecules not only pack in solids in similar manners, but

(22) Gavezzotti, A. *J. Am. Chem. Soc.* **1989**, *111*, 1835.
(23) Campbell, A. J.; Cottrell, C. E.; Fyfe, C. A.; Yannoni, C. S. *J. Am. Chem. Soc.* **1979**, *101*, 1351. Hanson, B. E.; Lisic, E. C.; Petty, J. T.; Iannacone, G. *Inorg. Chem.* **1984**, *23*, 4062. Dorn, H. C.; Hanson, B. E.; Motell, E. *J. Organomet. Chem.* **1982**, *224*, 181.
(24) Fyfe, C. A.; Wasylishen, R. E. In *Solid State Chemistry Techniques*; Cheetham, A. K., Day, P., Eds.; Clarendon Press: Oxford, 1987; Chapter 6, p 190. Fyfe, C. A. *Solid State NMR for Chemists*; CFC Press: Guelph, Ontario, Canada 1983.
(25) (a) Sourisseau, C.; Lucazeau, G.; Dianoux, A. J.; Poinsignon, C. *Mol. Phys.* **1983**, *48*, 367. (b) Chhor, K.; Lucazeau, G., Sourisseau, C. *J. Raman Spectrosc.* **1981**, *11*, 183. (c) Chhor, K.; Lucazeau, G. *J. Raman Spectrosc.* **1982**, *13*, 235. (d) Lucazeau, G.; Chhor, K.; Sourisseau, C.; Dianoux, A. J. *J. Chem. Phys.* **1983**, *76*, 307.
(26) On comparing E_a with ΔE values, it should be kept in mind that the activation energy is a mean value measured in a broad temperature range, while the potential energy barriers are dependent on the temperature at which diffraction data were collected. Since the activation energy integrates several effects (including correlated and uncorrelated jumping motion), only differences in order of magnitudes rather than a factor, e.g., of 2 or 3, are truly significant.
(27) Sanford, W. E.; Boyd, R. K. *Can. J. Chem.* **1976**, *54*, 2773. Boyd, R. K.; Fyfe, C. A.; Wright, D. A. *J. Phys., Chem. Solids* **1974**, *35*, 1355. Ok, J. H.; Vold, R. R.; Vold, R. I.; Etter, M. C. *J. Phys. Chem.* **1989**, *93*, 7618.
(28) Gavezzotti, A.; Simonetta, M. *Acta Crystallogr. Sect. A* **1975**, *31*, 165.
(29) Anderson, S. E. *J. Organomet. Chem.* **1974**, *71*, 263.
(30) Delise, P.; Allegra, G.; Mognaschi, E. R.; Chierico, A. *J. Chem. Soc., Faraday Trans. 2* **1975**, *71*, 207.
(31) Allen, P. S.; Cowking, A. *J. Chem. Phys.* **1967**, *47*, 4286.
(32) Aime, S.; Braga, D.; Gobetto, R.; Grepioni, F.; Orlandi, A.; *Inorg. Chem.* **1991**, *30*, 951.
(33) Braga, D.; Grepioni, F. Unpublished results.

also show similar dynamic behavior, suggests that the crystal building process (at least for small organic and organometallic molecules in the absence of strong directional intermolecular interactions) is essentially a process of molecular self-assembling based on the *shape* of the molecules or component fragments.

Acknowledgment. Financial support by Ministero della Università e della Ricerca Scientifica e Tecnologica is acknowledged.

Registry No. C_6H_6, 71-43-2; C_6Me_6, 87-85-4; $(C_6H_6)_2Cr$, 1271-54-1; $(C_6H_6)Cr(CO)_3$, 12082-08-5; $(C_6Me_6)Cr(CO)_3$, 12088-11-8; $(1,3,5\text{-}C_6H_3Me_3)Mo(CO)_3$, 12089-15-5.

Reactions of $[Cp^*RuOMe]_2$. 7.† Intramolecular Transformation of a $RuOCH_3$ Unit into a Ru(CO)H Unit: Crystal and Molecular Structure of $Cp^*Ru(\mu\text{-}H)_2(\mu\text{-}CO)RuCp^*$

Byung-Sun Kang,‡ Ulrich Koelle,*,‡ and Ulf Thewalt§

Institute for Inorganic Chemistry, Technical University of Aachen, W-5100 Aachen, FRG, and Center of X-ray Crystallography, University of Ulm, W-7900 Ulm/Donau, FRG

Received April 23, 1990

Electrophilic ($(Me_3Si)_2NH$) as well as nucleophilic (H^-) degradation of $[Cp^*RuOMe]_2$ (1) ($Cp^* = \eta^5\text{-}C_5Me_5$) affords high yields of the dimeric carbonyl hydride $Cp^*Ru(\mu\text{-}H)_2(\mu\text{-}CO)RuCp^*$ (2). The course of the reaction is elucidated by labeling 1 with $^{13}CD_3O$ or $^{12}COD_3$, and it is shown that both CO and the bridging hydrides in 2 originate from the OMe group in 1. The molecular structure of 2, determined by single-crystal X-ray diffraction (space group, *Pa*, a = 12.621 (3) Å, b = 8.574 (2) Å, c = 10.089 (2) Å, β = 108.56 (3)°, Z = 2), shows close similarity to that of the related tetrahydride $Cp^*Ru(\mu\text{-}H)_4RuCp^*$ (3) with nearly identical cell parameters and Ru≡Ru distances (2.444 Å in 2, 2.463 (1) Å in 3).

Alkoxo derivatives of the late transition metals offer an interesting pattern of reactivities.[1] Alkoxide transfer, electrophilic as well as nucleophilic substitution, insertion into the M–OR bond, and β-hydrogen abstraction with formation of hydrides are among the reactions studied. Aldehyde elimination in some cases occurs directly in the course of nucleophilic exchange of e.g. halide for alkoxide so as to give the hydride as the sole product.[2] A free coordination site has been presumed as a prerequisite for those hydrogen-transfer reactions.[1]

The dimeric alkoxo complex $[Cp^*RuOMe]_2$[3,4] (1), despite its coordinative unsaturation (16 VE), is thermally stable under an inert atmosphere to about 90 °C. Aldehyde elimination with formation of a hydride was observed at 60 °C in the presence of strongly coordinating 1,5-cyclooctadiene.[5] When 1 is treated with electrophilic or nucleophilic reagents that cleave one methoxo group from the dimer, C–H bond activation of the residual methoxo group, leading to the dimeric carbonyl hydride 2, is observed and is described as follows.

Results

Reaction with $(Me_3Si)_2NH$. Refluxing $[Cp^*RuOMe]_2$ with a molar quantity of hexamethyldisilazane in hexane (eq 1) affords, after cooling, the known complex 2[6] in up to 90% yield by direct crystallization from the reaction mixture.

$$\underset{1}{[Cp^*RuOMe]_2} + (Me_3Si)_2NH \xrightarrow[\text{reflux, 12 h}]{n\text{-hexane}} \underset{2}{Cp^*Ru(\mu\text{-}H)_2(\mu\text{-}CO)RuCp^*} + Me_3SiOMe + Me_3SiNH_2 \quad (1)$$

Rhombic plates of 2 crystallize from the concentrated solution. The compound is readily identified by a high-field hydridic absorption at δ −12.98 in the ^1H NMR spectrum and by a characteristic band at 1793 cm^{-1} in the infrared spectrum, in agreement with the data of ref 6.

Hydrido carbonyl complex 2 has been obtained as the photolysis product of the corresponding dicarbonyl $[Cp^*Ru(CO)(\mu\text{-}H)]_2$ (4).[6] Apart from reaction 1, we did observe the compound as one of the reaction products of 1 with diolefins, e.g. 1,3-cyclohexadiene, and with various olefinic alcohols. Finally, it is isolated as one of the products from the thermal decomposition of 1 (see below).

The diversity of reactions that lead to 2 suggests this molecule to form a deep pitch in the Cp*Ru–H–CO reaction surface. Reaction 1 in particular provides an easy, high-yield access to 2 from readily prepared 1,[3d] which may

† Part 6: See ref 3d.
‡ Technical University of Aachen.
§ University of Ulm.

(1) For a review see: Bryndza, H. E.; Tam, W. *Chem. Rev.* **1988**, *88*, 1163.
(2) (a) Ros, R.; Michelin, R. A.; Bataillard, R.; Roulet, R. *J. Organomet. Chem.* **1978**, *161*, 75. (b) Park, S.; Roundhill, D. M.; Rheingold, A. L. *Inorg. Chem.* **1987**, *26*, 3974. (c) Bennett, M. A. *J. Organomet. Chem.* **1986**, *300*, 7. (d) Yoshida, T.; Otsuka, S. *J. Am. Chem. Soc.* **1977**, *99*, 2134. (e) Diamond, S. E.; Mares, F. *J. Organomet. Chem.* **1977**, *142*, C55. (f) Arnold, D. P.; Bennett, M. A. *J. Organomet. Chem.* **1980**, *199*, C17. (g) Milstein, D.; Calabrese, J. C. *J. Am. Chem. Soc.* **1982**, *104*, 3773. (h) Arnold, D. P.; Bennett, M. A. *Inorg. Chem.* **1984**, *23*, 2110. (i) Fernández, M. J.; Esteruelas, M. A.; Covarrubias, M.; Oro, L. A. *J. Organomet. Chem.* **1986**, *316*, 343.
(3) (a) Koelle, U.; Kossakowski, J. *J. Chem. Soc., Chem. Commun.* **1988**, 549. (b) Koelle, U.; Kossakowski, J. *J. Organomet. Chem.* **1989**, *362*, 383. (c) Koelle, U.; Kossakowski, J.; Boese, R. *J. Organomet. Chem.* **1989**, *378*, 449. (d) Koelle, U.; Kossakowski, J. *Inorg. Synth.*, in press. (e) Koelle, U.; Kossakowski, J.; Raabe, G. *Angew. Chem., Int. Ed. Engl.* **1990**, *29*, 773.
(4) Loren, S. D.; Campion, B. K.; Heyn, R. H.; Don Tilley, T.; Bursten, B. E.; Luth, K. W. *J. Am. Chem. Soc.* **1989**, *111*, 4712.
(5) Koelle, U.; Kang, Byung-Sun; Raabe, G.; Krüger, C. *J. Organomet. Chem.* **1990**, *386*, 261.
(6) Forrow, N. J.; Knox, S. A. *J. Chem. Soc., Chem. Commun.* **1984**, 679.

0276-7333/91/2310-2569$02.50/0